Transactions, SMiRT-22
San Francisco, California, USA - August 18-23, 2013
Division III

MULTISCALE NUCLEAR FUEL ANALYSIS VIA ASYMPTOTIC EXPANSION HOMOGENIZATION

J. D. Hales[1], M. R. Tonks[1], K. Chockalingam[2], D. M. Perez[1], S. R. Novascone[1], B. W. Spencer[1], and R. L. Williamson[1]

[1] Idaho National Laboratory, Idaho Falls, ID (jason.hales@inl.gov)
[2] Interdisciplinary Centre for Advanced Materials Simulation (ICAMS), Ruhr University Bochum, Germany

ABSTRACT

Multiscale analysis aims to improve predictions at the macro-scale by utilizing high-fidelity models running at a lower length-scale. The lower length-scale models provide a detailed view of the material behavior that is used to determine the average material response to be used at the macro-scale. This approach is especially useful in the nuclear field, since irradiation experiments are difficult and expensive to conduct. The lower length-scale models complement the experiments, reducing the total number of experiments that are needed. Multiscale modeling is a critical part of the BISON-MARMOT fuel performance codes being developed at Idaho National Laboratory (Williamson et al. (2012), Tonks et al. (2010)).

One critical aspect of multiscale modeling is the ability to extract the relevant information from the lower length-scale simulations. One approach, the asymptotic expansion homogenization (AEH) technique (Guedes et al. (1990), Ghosh et al. (1995), Hassani and Hinton (1998), Laschet and Apel (2010), and Oliviera et al. (2011)), has proven to be an effective method for determining homogenized material parameters. The AEH technique prescribes a system of equations to solve at the micro-scale that are used to compute homogenized material constants for use at the macro-scale.

In this work, we employ AEH to explore the effect of evolving microstructural thermal conductivity on nuclear fuel performance. This builds on the work of Tonks et al. (2010) and Williamson et al. (2012), where a direct calculation was used to obtain average thermal conductivity. We show that the AEH approach fits cleanly into the BISON and MARMOT codes and provides a natural, multidimensional homogenization capability.

INTRODUCTION

In UO_2 fuel for LWRs, the radiation environment affects thermal conductivity, swelling, densification, creep, and fission gas production and release. At the engineering scale, empirical models are employed that follow the observable trends in experimental data. As an example, the Fink-Lucuta model of thermal conductivity (Fink (2000) and Lucuta et al. (1996)) is a function of temperature and burnup. In reality, the evolving thermal conductivity is due to many phenomena occurring at lower length-scales such as solid and gaseous fission product generation, fission product diffusion, void formation, and crack formation.

Conducting nuclear fuel experiments provides essential, fundamental data for understanding the behavior of fuel, cladding, and other components. This data may be analyzed in an effort to create or improve an empirical engineering scale model. These experiments are, however, difficult and expensive to perform due to the inherent radioactivity involved.

Conducting computational experiments has many advantages. Through computer modeling, geometries, initial conditions, boundary conditions, and material models can be analyzed relatively quickly and inexpensively. It is also possible to feed numerical solutions from lower length-scale

analyses to engineering scale calculations. In this way, we may inform macro-scale analyses with meso-scale or micro-scale information. It is thus viable to develop a thermal conductivity model that is based on fission product formation and diffusion, void formation, etc.

AEH based on the finite element method is ideally suited for this problem, as it can seamlessly couple the macro- and micro-scale together by passing the homogenized property to the continuum scale. As mentioned, the microstructure is constantly evolving and, hence, so is the macro-scale thermal conductivity. In the current work, AEH is used with the phase field method (Chen (2002)), which captures the evolving characteristics of the meso-scale structure. Thereby, AEH concurrently computes the thermal conductivity of this complex system as the simulation progresses.

It is noted that the microstructure under consideration is assumed to have the same temperature at every point. It is conventional to make such an approximation provided the thermal gradient is not steep. In case of steep thermal gradients, nonlinear AEH methods (Chung et al. (2001)) are employed, and the temperature need not be the same at every point in the microstructure.

The fuel simulation codes BISON and MARMOT, under development at Idaho National Laboratory, have been built with this vision of multiscale modeling in mind. BISON is a multidimensional nuclear fuel performance analysis code capable of running in 1D, 2D, or 3D. It is applicable to the analysis of LWR fuel, TRISO-coated fuel particles, and metal fuels. Its capabilities include a selection of fuel and cladding thermal and mechanical material models, fission gas release, thermal and mechanical contact, evolving gap conductivity and pressure, axial and radial power scaling, fuel densification and swelling, and other models. It is possible to run BISON coupled with a neutronics code.

MARMOT is a multiphysics meso-scale simulation code focused on modeling the coevolution of microstructure and material properties. In MARMOT, the system of phase field partial differential equations (PDEs) is solved simultaneously with PDEs defining additional physics such as heat conduction and solid mechanics. The PDEs are solved via the finite element method with implicit time integration, taking advantage of advanced tools such as automatic mesh and time step adaptivity. MARMOT has been used to model various microstructural phenomena, ranging from grain boundary migration to bubble growth and coalescence.

Both BISON and MARMOT are built on the MOOSE (Gaston et al. (2009)) framework. Both codes solve their equations in a fully-coupled manner by means of the Jacobian-free Newton-Krylov method (Knoll et al. (2004)). They run efficiently on parallel computers.

The following section reviews the AEH technique as applied to thermal conductivity. Next is a section reviewing solutions to standard benchmark problems from the literature. That is followed by a discussion of mesh convergence. The next section presents results applicable to nuclear fuel simulation. The final section gives conclusions and a discussion of future work.

ASYMPTOTIC EXPANSION HOMOGENIZATION

Consider the following partial differential equation used for heat conduction:

$$\frac{\partial}{\partial x_i^e}\left(a_{ij}\frac{\partial}{\partial x_j^e}\right)u^e = f. \tag{1}$$

The superscript indicates that the solution u^e incorporates macro-scale and micro-scale information. Leaving the derivation details to the referenced papers, the asymptotic expansion homogenization technique involves two systems of equations. One is based on the micro-scale, represents the repeating microstructure, and requires periodic boundary conditions to enforce the periodicity of the structure. The second is at the macro-scale and represents the same partial differential equation as Eq. 1 but with homogenized material constants a_{ij}^H replacing a_{ij} and u and x replacing u^e and x_i^e.

The equation to be solved at the micro-scale is

$$\int_Y \frac{\partial v}{\partial y_i} k_{ij} \frac{\partial \psi^k}{\partial y_j} \mathrm{d}\boldsymbol{y} = \int_Y \frac{\partial v}{\partial y_i} k_{ik} \, \mathrm{d}\boldsymbol{y} \; \forall \; v_i \in V_Y. \tag{2}$$

With ψ^k known, the homogenized thermal conductivity k_{ij}^h is computed as

$$k_{ij}^h = \frac{1}{|Y|} \int_Y k_{ik} \left(\boldsymbol{I} - \frac{\partial \psi^j}{\partial y_k} \right) \mathrm{d}\boldsymbol{y}. \tag{3}$$

This homogenized thermal conductivity is used at the macro-scale.

For elasticity, a similar pair of expressions exist to find the homogenized elastic constants to be used at the macro-scale. The periodic equation at the micro-scale in the case of elasticity is

$$\int_Y \frac{\partial v_i}{\partial y_j} D_{ijkl} \frac{\partial \chi_k^{mn}}{\partial y_l} \mathrm{d}\boldsymbol{y} = \int_Y \frac{\partial v_i}{\partial y_j} D_{ijkl} \, \mathrm{d}\boldsymbol{y} \; \forall \; v_i \in V_Y. \tag{4}$$

The homogenized elasticity tensor D_{ijkl}^h is then

$$D_{ijkl}^h = \frac{1}{|Y|} \int_Y D_{ijkl} \left(\boldsymbol{I} - \frac{\partial \chi_k^{mn}}{\partial y_l} \right) \mathrm{d}\boldsymbol{y}. \tag{5}$$

A key point to understand is the fact that the RHS of Eq. 2 and 4 represents not a single vector field but a set of vector fields. This implies that ψ and χ represent sets of solution vectors. Specifically, for three dimensions, ψ holds three solutions and χ holds six.

STANDARD BENCHMARK PROBLEM RESULTS

In order to show that the implementation of this technique is correct, the results obtained using BISON/MARMOT are compared to standard problems. For heat conduction, consider a simple unit cube domain divided equally along the x-axis into halves. One half has a thermal conductivity of 10 and the other half has a thermal conductivity of 100. The analytic solution for the homogenized thermal conductivity in the x direction is found by summing the thermal resistance, recognizing that the halves are in series.

$$R_x = \frac{L}{Ak_x} = R_1 + R_2 = \frac{L_1}{A_1 k_1} + \frac{L_2}{A_2 k_2} = \frac{0.5}{1 \cdot 10} + \frac{0.5}{1 \cdot 100} \tag{6}$$

where R is resistance, L is length, A is area, and the subscripts represent each of the two materials. Since in this case the length and area have magnitude one, k_x = 18.1818.

The analytic solution for the homogenized thermal conductivity in the y direction is found similarly with the recognition that the halves are in parallel.

$$\frac{1}{R_y} = \frac{Ak_y}{L} = \frac{1}{R_1} + \frac{1}{R_2} = \frac{0.5 \cdot 10}{1} + \frac{0.5 \cdot 100}{1} \tag{7}$$

Thus, k_y = 55.0. BISON/MARMOT compute these analytic solutions exactly using the AEH approach.

For an elasticity demonstration, we consider the so-called short fiber and long fiber problems defined in Ghosh et al. (1995). These problems involve square, periodic domains containing fiber and matrix materials. The geometry for these problems is shown in Figure 1.

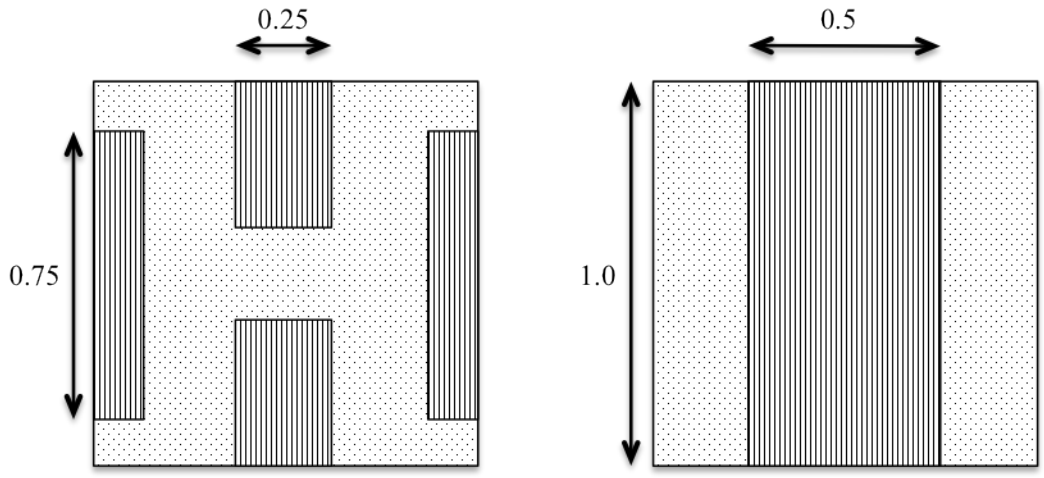

Figure 1. Short fiber (left) and long fiber (right) geometries. Figure reproduced from Ghosh et al. (1995).

The fiber portion of the problem is defined with a Young's modulus of 400 GPa and a Poisson's ratio of 0.2. The matrix portion is defined with a Young's modulus of 72.5 GPa and a Poisson's ratio of 0.33.

The AEH technique was used in BISON/MARMOT to compute the four unique homogenized elasticity tensor entries (1111, 2222, 1212, and 1212) for these problems. The four values were obtained using Eq. 5 and the four solution vectors in χ computed from Eq. 4. The results are compared to data given in Ghosh et al. (1995) in Table 1 for the short fiber problem and Table 2 for the long fiber problem. The results obtained by BISON/MARMOT match the reported data very well.

Table 1: Elasticity constants for the short fiber problem. Data for the last four columns taken from Ghosh et al. (1995). BISON/MARMOT results are very close to the HOMO2D and Fish and Wagiman solutions.

	BISON/MARMOT	VCFEM	HOMO2D	Fish and Wagiman (1992)	Self consistent
E1111 (GPa)	122.457	118.807	122.4	122.457	132.491
E2222 (GPa)	151.351	139.762	151.2	151.351	205.753
E1212 (GPa)	42.112	42.440	42.10	42.112	51.384
E1122 (GPa)	36.191	38.052	36.23	36.191	36.191

Table 2: Elasticity constants for the long fiber problem. Data for the last four columns taken from Ghosh et al. (1995). BISON/MARMOT results are very close to the HOMO2D and Fish and Wagiman solutions.

	BISON/MARMOT	VCFEM	HOMO2D	Fish and Wagiman (1992)	Self consistent
E1111 (GPa)	136.138	136.137	136.1	136.147	165.548
E2222 (GPa)	245.810	245.810	245.8	245.81	247.575
E1212 (GPa)	46.8498	46.8498	46.85	46.85	64.887
E1122 (GPa)	36.076	36.076	36.08	36.076	42.048

MESH CONVERGENCE

Finite element solutions are more accurate with finer meshes, and this characteristic applies to AEH simulations. However, the method does not inherently require very fine meshes for accurate solutions. To demonstrate, consider the matrix and fiber model shown in Figure 2. This model was run with increasingly fine meshes to show how the elasticity constants change with mesh refinement. The material properties for the matrix and fiber constituents are the same as for the short and long fiber problems of the previous section. As with all AEH simulations, periodic boundary conditions are applied on opposite faces.

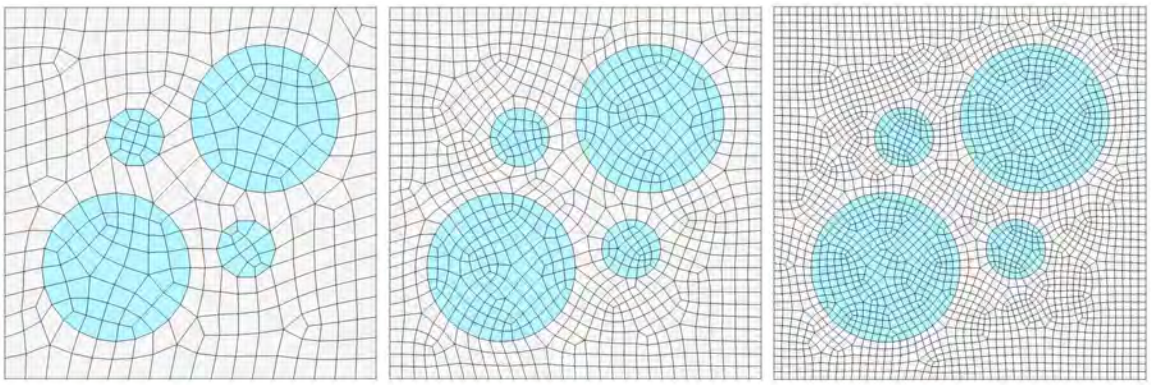

Figure 2. Meshes used in the mesh convergence study with 398, 1092, and 2697 nodes.

As can be seen in Figure 3, the elasticity constants vary little beyond about 1000 nodes per mesh. It is also worth noting that due to the symmetry of this example, we would expect the E1111 and E2222 constants to be equal. At about 1000 nodes, these quantities match. This simple demonstration shows that the AEH technique can provide useful data without overly fine meshes and large computational expense.

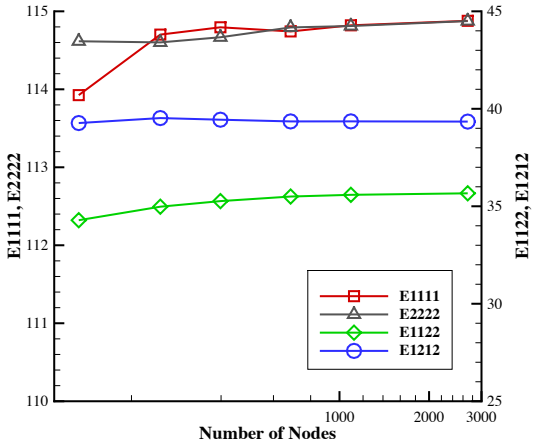

Figure 3. Elasticity constants with mesh refinement. The constants vary little beyond ~1000 nodes.

APPLICATION TO NUCLEAR FUEL SIMULATIONS

The effect of hydrides on cladding performance is an important concern in regards to in-reactor behavior and long term storage of nuclear fuel. In particular, an increasing hydride concentration reduces the ductility of the cladding. Furthermore, the cladding becomes more susceptible to cracking as hydrides reorient from a circumferential arrangement to a radial one.

Given the expense of testing irradiated cladding specimens with hydride inclusions, it is attractive to consider numerical tools that may provide insight into cladding/hydride behavior. Rashid et al. (2009) have developed a constitutive model based on relating the response of circumferential and radial hydrides with the Zircaloy behavior. The aim in that work is to provide a means of predicting cladding failure.

In contrast to that advanced approach, the AEH technique provides a simple and inexpensive way of understanding inhomogeneous material such as cladding with hydrides. The example shown here is not meant to be representative of an actual cladding specimen, but it does show that the AEH procedure can give insight beyond simple assumptions and has the potential to give much more accurate and predictive data.

We take as our model a cladding/hydride composite where the hydrides are modeled as inclusions in the model. For simplicity, a single inclusion shape is replicated and placed randomly in the matrix. The material constants for the matrix are: Young's modulus, 75 GPa; Poisson's ratio, 0.3. The material constants for the inclusions are: Young's modulus, 140 GPa; Poisson's ratio, 0.27.

Four analyses were completed. The fraction of inclusions in each analysis was approximately 1%, 2%, 4%, and 8% by area in plane strain conditions. The AEH technique was used to compute the four elasticity constants for the homogenized elasticity tensor. Figure 4 shows the results, where the resulting constants are normalized by the value of the constants computed by an elementary volume average.

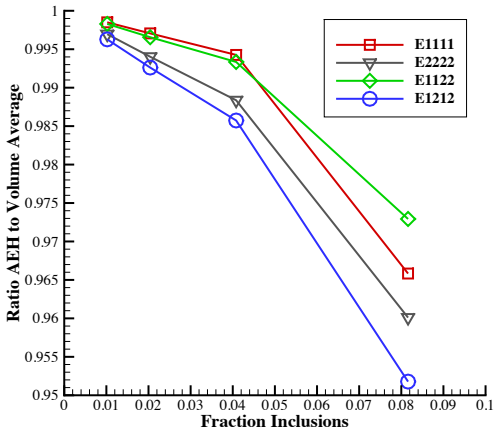

Figure 4. Elasticity constants for a Zircaloy matrix with hydride inclusions normalized by volume averaged values.

Note that the elasticity constants do not vary considerably from volume averaged values when the fraction of inclusions is low. However, the difference grows with increasing fraction of inclusions and is considerably different at an 8% inclusion fraction. Furthermore, the rate of change in the difference increases with increasing inclusion fraction. This indicates that the simplest approaches to considering the complete system, namely volume averaging the material constants, must be undertaken with caution. The AEH approach, however, is an extremely efficient approach that can be expected to provide more accurate results.

Despite the simplicity of this model, it shows something of the potential of the AEH technique for investigating cladding behavior. Further enhancements might include a study of the effect of orientation on the overall response; the effect of a statistical variation in inclusion properties; behavioral changes given additional oxide inclusions; and the effect of inclusion shape and size. Additional studies are warranted.

In Williamson et al. (2012), MARMOT and BISON were coupled in a multiscale analysis. BISON computed macro-scale temperature and neutron flux. These quantities were passed to MARMOT, which ran a thermal conductivity simulation. This meso-scale simulation tracked bubble nucleation and growth. A steady-state heat conduction calculation then computed thermal conductivity based on this evolving meso-scale system. The thermal conductivity was returned to BISON for its use at the macro-scale.

The following example problem is patterned after this MARMOT calculation for thermal conductivity. As before, MARMOT calculates meso-scale bubble evolution, which affects local thermal conductivity. A homogenized thermal conductivity is computed as an applied flux times the length of the domain divided by the average change in temperature over that length. This direct calculation is accompanied by the AEH calculation of the thermal conductivity according to Eq. 2 and 3.

A typical local thermal conductivity distribution can be seen in Figure 5. It is this local thermal conductivity that serves as input to the direct and AEH homogenization techniques. Note that the thermal conductivity varies widely. Note also the adaptively refined mesh and the fact that periodic boundary conditions have been enforced.

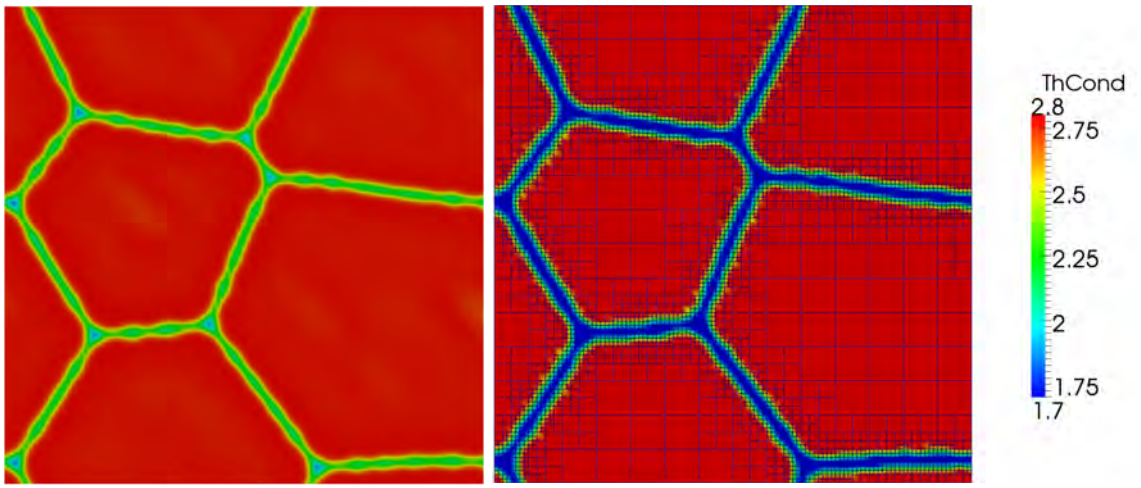

Figure 5. On the left, grains and grain boundaries with bubbles forming. On the right, local thermal conductivity as computed by MARMOT. The thermal conductivity is low at grain boundaries and bubbles. Note the locally refined mesh.

A plot comparing the homogenized thermal conductivity computed by the direct approach and the AEH approach appears in Figure 6. Note that the direct approach and the AEH approach give similar but not identical solutions. The direct method is very sensitive to bubbles existing on the boundary where the flux is applied. Since the thermal conductivity is calculated from the average temperature on that side, if a bubble forms on the grain boundary, thus locally lowering the temperature, it can significantly affect the prediction. See Figure 7 for an example. The AEH method is not sensitive to such local details. Toward the end of the analysis, the thermal conductivity drops to near zero as the grains become isolated from one another and the bubble fraction grows.

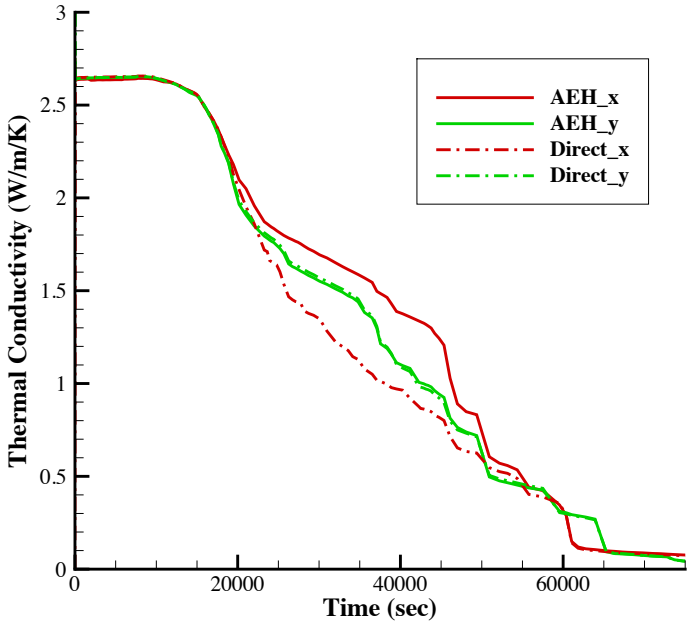

Figure 6. Homogenized thermal conductivity vs. time for the AEH and direct techniques.

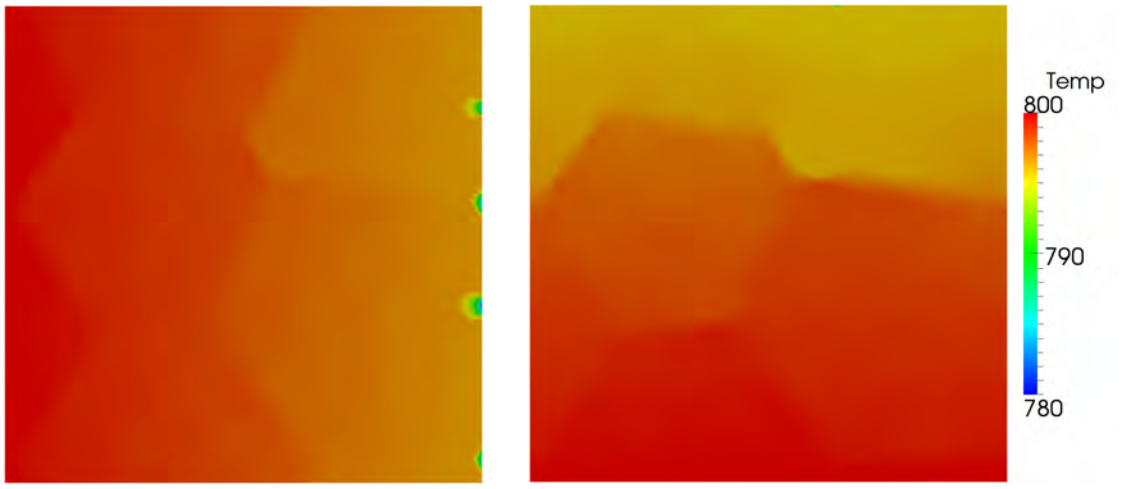

Figure 7. Temperature from the direct approach with a flux applied in the x-direction (left) and y-direction (right) at approximately 40000 seconds. Note the areas of low temperature on the right edge of the x-direction plot. These correspond to bubble locations and account for the lower thermal conductivity computed by the direct approach.

The AEH approach gives satisfactory results for this thermal conductivity analysis. It has a low computational overhead and is straightforward to implement. In addition, the technique has a consistent approach for thermal conductivity and elasticity homogenization.

CONCLUSIONS

Asymptotic expansion homogenization has a strong history of development in the mathematical and engineering fields. It is applicable for homogenization of thermal conductivity, elasticity constants, and other quantities. It has a low computational expense (the same as steady state heat conduction or linear elasticity) and is straightforward to implement. It is thus a vehicle for enabling multiscale analysis.

The AEH technique has been implemented in BISON/MARMOT where it has been shown to solve standard benchmark problems accurately. It has also been shown to give good results without overly fine meshes.

Possible nuclear fuel analysis applications of the technique include estimating the mechanical response of cladding tubes that have hydride inclusions. The technique is also applicable to computing homogenized thermal conductivity in nuclear fuel.

Future work with AEH in BISON/MARMOT will focus on better understanding the meso-scale to macro-scale coupling in nuclear fuel and cladding. It is anticipated that the technique will prove to be a robust and accurate way to inform macro-scale models of lower length-scale evolution.

ACKNOWLEDGEMENTS

The submitted manuscript has been authored by a contractor of the US Government under Contract DE-AC07-05ID14517. Accordingly, the US Government retains a non-exclusive, royalty free license to publish or reproduce the published form of this contribution, or allow others to do so, for US Government purposes.

REFERENCES

Williamson, R. L., Hales J. D., Novascone, S. R., Tonks, M. R., Gaston D. R., Permann, C. J., Andrs, D. and Martineau, R. C. (2012). "Multidimensional multiphysics simulation of nuclear fuel behavior," *Journal of Nuclear Materials*, 423:149–63.

Tonks, M., Gaston, D., Permann, C., Millett, P., Hansen, G., and Wolf, D. (2010). "A coupling methodology for mesoscale-informed nuclear fuel performance codes," *Nucl. Engrg. Design*, 240(10):2877–2883.

Guedes, J.M., Kikuchi, N. (1990). "Preprocessing and postprocessing for materials based on the homogenixation method with adaptive finite element methods," *Computer Methods in Applied Mechanics and Engineering*, 83(2):143–198.

Ghosh, S., Lee, K., and Moorthy, S. (1995). "Multiple scale analysis of heterogeneous elastic structures using homogenization theory and voronoi cell finite element method," *Internat. J. Solids Structures*, 32(1):27– 62.

Hassani, B. and Hinton, E. (1998). "A review of homogenization and topology optimization I–homogenization theory for media with periodic structure," *Computers & Structures*, 69:707–717.

Laschet, G. and Apel, M. (2010). "Thermo-elastic homogenization of 3-d microstructure simulated by the phase-field method," *Steel Research International*, 81:637–643.

Oliviera, J. A., Pinho-da-Cruz, J. and Teixeira-Dias, F. (2011). *Advances in Composite Materials – Analysis of Natural and Man-Made Materials*, chapter 23. InTech.

Fink, J. K. (2000). "Thermophysical properties of uranium dioxide," *Journal of Nuclear Materials*, 249:1–18.

Lucuta, P. G., Matzke, H. J., and Hastings, I. J. (1996). "A pragmatic approach to modeling thermal conductivity of irradiated UO_2 fuel: review and recommendations," *Journal of Nuclear Materials*, 232:166–180.

Chen, L.Q. (2002). "Phase-Field Models for Microstructure Evolution," *Annual Review of Materials Research*.

Chung, P. W., Tamma, K. K., and Namburu, R. R. (2001). "Homogenization of temperature-dependent thermal conductivity in composite materials," *Journal of Thermophysics and Heat Transfer*, 15:10-17.

Gaston, D., Newman, C., Hansen, G., and Lebrun-Grandie, D. (2009). "MOOSE: A parallel computational framework for couple systems of nonlinear equations," *Nuclear Engineering and Design*, 239(10):1768-1778.

Knoll, D. A. and Keyes, D. E. (2004). "Jacobian-free Newton-Krylov methods: A survey of approaches and applications," *Journal of Computational Physics*, 193(2):357-397.

Rashid, J., Rashid, M., Machiels, A., and Dunham, R (2009). "A New Material Constitutive Model for Predicting Cladding Failure," Proceedings of Top Fuel, Paris, France.